Steel and Composite Structures, Vol. 1, No. 1 (2001) 33-50
DOI: http://dx.doi.org/10.12989/scs.2001.1.1.033

Experimental study on the cyclic behaviour of bolted end-plate joints

Sándor Ádány†

Department of Structural Mechanics, Budapest University of Technology and Economics, Hungary

Luis Calado‡

DECivil, Instituto Superior Técnico, Lisbon, Portugal

László Dunai‡

Department of Steel Structures, Budapest University of Technology and Economics, Hungary

Abstract. In this paper an experimental study is performed on end-plate type joints. The test arrangement represents a column-base joint of a steel frame. Altogether six specimens were tested, each of them subjected to cyclic loading. The specimens were carefully designed by performing detailed preliminary calculations so that they would present typical behaviour types of end-plate joints. On the basis of the experimentally established moment-rotation relationship, the cyclic characteristics of each specimen have been calculated and compared to one another. The results are evaluated, qualitative and quantitative conclusions are drawn.

Key words: experimental testing; bolted connections; joints; cyclic behaviour; hysteresis loops; failure mode; beam-column joints.

---

1. Introduction

End-plate-type joints are widely used in steel frame structures. These joints can connect either two steel elements (such as beam-to-column, beam-to-beam or column-to-column joints) or a steel and a concrete/reinforced concrete element (like column-base joints or joints of a steel beam and a reinforced concrete column). The main advantage of this type of joint is in the production and mounting; at the same time, however, their application results in a more complicated structural behaviour and, consequently, requires more complex design.

In the past decade a great deal of investigation (both numerical and experimental) has been performed to analyse the behaviour of the different kinds of end-plate joints, and to develop appropriate numerical models for everyday engineering practice. As a result of these investigations, focused mainly on monotonic behaviour, calculation methods have been developed and introduced

†Assistant
‡Associate Professor

to the new European steel code for steel-to-steel joints (Eurocode 3 1993). Also design tables have been worked out for column-bases (Wald *et al.* 1994). To cyclic behaviour, however, much less effort has been devoted. Nevertheless, a certain number of experimental programs have been performed (Dunai *et al.* 1996, Calado *et al.* 1999, Ballio *et al.* 1997, Calado and Lamas 1998, Calado *et al.* 1998), and some numerical models have been developed as well (Ádány and Dunai 1995, Ádány and Dunai 1997, Dunai 1992, Dunai *et al.* 1995, Dunai and Ádány 1997). The lack of appropriate numerical models can be explained by the rather complicated joint behaviour which requires sophisticated models and time-consuming calculations.

A more complete understanding of the cyclic behaviour of end-plate joints is essential, especially in the seismic design. The importance of the problem was clearly demonstrated during the recent earthquake events of Northridge and Kobe, where significant structural damage of steel frames took place in the connection zones in several cases. Thus, it is important to be able to simply but reliably asses the behaviour of the joints in case of seismic actions, in order to satisfy the required resistance, rigidity, ductility and energy absorption demands.

In this paper an experimental program is reported, carried out in the Instituto Superior Técnico, Lisbon, Portugal is reported. The test program is devoted to the cyclic behaviour of column-base type end-plate joints. The paper presents the whole process of the experimental program. In Section 2, the aim of the program is defined, in Section 3, the preliminary work is summarised; and in Section 4, the results are presented. Finally, some conclusions are drawn.

2. Aim

According to previous experiments, four basic behaviour components can be distinguished which determine the joint behaviour, usually measured by the moment-rotation relationship. These components, illustrated in Fig. 1, are the following:

- end-plate behaviour, due to elastic/plastic deformation of the end-plate,
- bolt behaviour, due to elastic/plastic elongation of bolts,
- steel beam/column behaviour, due to elastic/plastic deformations of the connected steel element, including local buckling,
- concrete behaviour, characterised by deterioration of the concrete element.

It should be noted that other reasons for failure also exist, like weld failure. It is reasonable to assume, however, that these phenomena have no significant effect on the behaviour before the failure. Furthermore they can be eliminated by appropriate design and fabrication.

The primary aim of the experimental program is to provide information on joint behaviour, including:

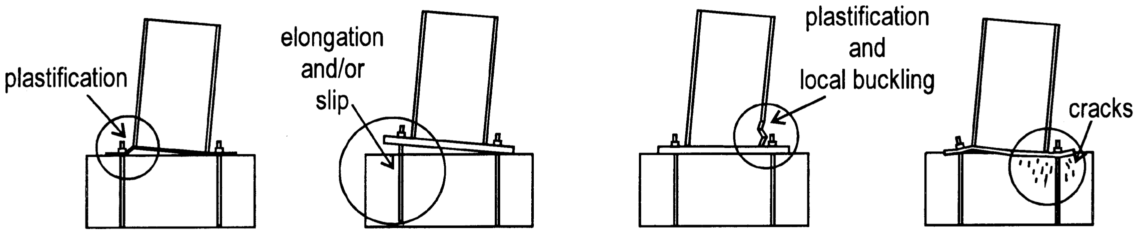

Fig. 1 Behaviour components of the joint behaviour

- joint behaviour governed by the *end-plate behaviour,*
- joint behaviour governed by the *bolt behaviour,*
- joint behaviour governed by the *beam/column behaviour,*
- joint behaviour governed by the *interaction of these elements.*

It is important to underline that concrete behaviour is not within the scope of this study.

The experimental data, provided by the tests, can also be used to verify and calibrate numerical models, which is another important aim of the experimental program.

3. Design of the tests

3.1. Test equipment

The test equipment is basically developed to test beam-to-column joints of steel frames. The global arrangement is illustrated in Fig. 2. In addition, there is a lateral frame to provide lateral support of the specimen, and avoid lateral movement or twisting. The whole testing process is managed by a personal computer, by means of a data acquisition unit which commands the actuator and reads the data from the load cell and displacement transducers. It is also important to note that displacement control is used. (More information about the test equipment can be found in Ferreira 1994 and Calado and Mele 1999.)

In designing the test, the specimen characteristics are determined in accordance with the parameters of the existing test set-up, by considering the geometrical properties, the load capacity of the actuator and load cell, as well as the displacement capacity of the inductive displacement transducers. The global arrangement is presented in Figs. 2 and 3, with the main geometrical dimensions of the specimens in Fig. 2. The arrangement represents a column base joint, with an H-shaped column and a practically rigid base. The application of the base element is necessary to be able to

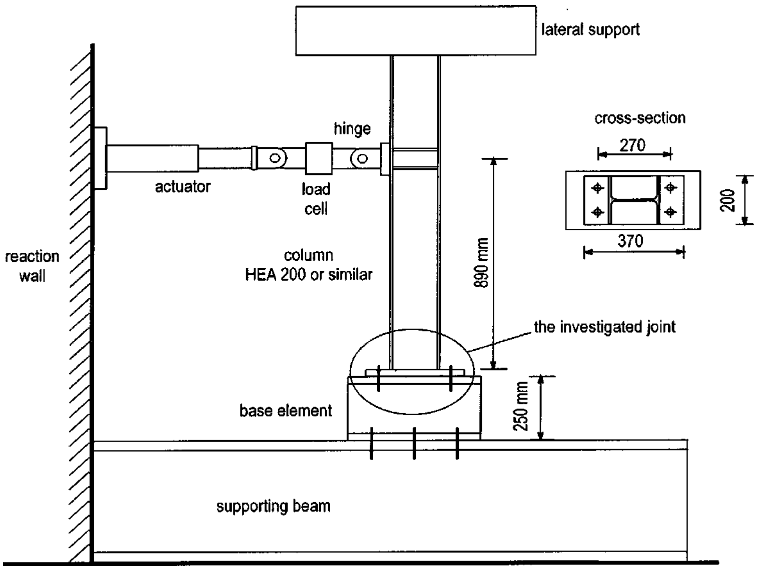

Fig. 2 Global arrangement with the main dimensions of the specimens

Fig. 3 Global arrangement of the test equipment

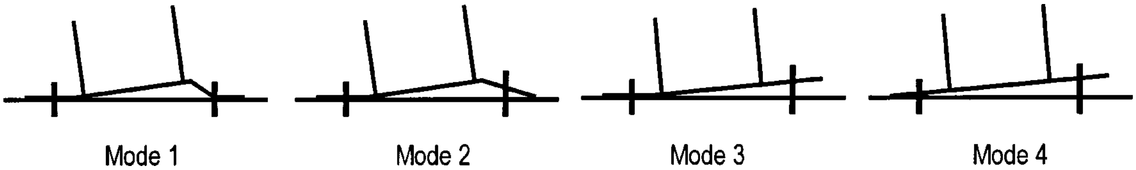

Fig. 4 Possible failure modes of end-plate joints

connect the column to the base beam. The top part of the specimen has the role of ensuring restraint against lateral movement and twisting of the column.

3.2. Preliminary calculations

To be able to achieve the intended phenomena of the specimens, preliminary calculations were done. The moment resistance of each joint was determined on two-dimensional models as the minimum of resistances belonging to the possible failure modes.

Four modes of failure were defined as illustrated in Fig. 4. Mode 1 represents the pure end-plate failure without failure of bolts. Mode 4 corresponds to the pure bolt failure, without any failure of the end-plate. Modes 2 and 3 are two cases of combined bolt and end-plate failure.

There are two potential places where plastic hinge (hinge-line) can be developed: either at the bolts, or at the column flange. The assumed positions of the plastic hinges are presented in Fig. 5.

The joint resistances belonging to the various failure modes can be expressed by the following formulae, for Modes 1 to 4, respectively.

$$M_{Rd,1} = M_{ep,Rd} \cdot 2 \cdot \left(1 + \frac{h'}{m'}\right) \tag{1}$$

$$M_{Rd,2} = M_{ep,Rd} \cdot \left(2 + \frac{h'}{m'+n}\right) + F_{b,Rd} \cdot \frac{h' \cdot n}{m'+n} \tag{2}$$

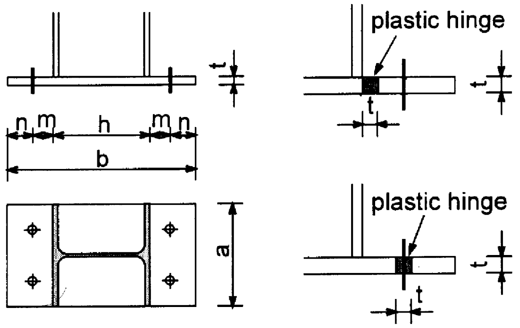

Fig. 5 Notations and assumed position of plastic hinges

$$M_{Rd,3} = M_{ep,Rd} + F_{b,Rd} \cdot (h' + m') \tag{3}$$

$$M_{Rd,4} = F_{b,Rd} \cdot b \tag{4}$$

The notations are as follow:

- $M_{ep,Rd}$ denotes the plastic resistance of the end-plate, calculated as:

$$M_{ep,Rd} = \frac{a \cdot t^2}{4} \cdot f_y \tag{5}$$

- $F_{b,Rd}$ denotes the plastic resistance of the bolts (two bolts), calculated as:

$$F_{b,Rd} = 2 \cdot A_b \cdot f_{yb} \tag{6}$$

- h' and m' can be calculated as:

$$h' = h + t \tag{7}$$

$$m' = m - \frac{t}{2} \tag{8}$$

- a, b, h, m, n, and t are geometrical dimensions of the joint, presented in Fig. 5;
- A_b is the sectional area of one bolt;
- f_y and f_{yb} the yield stress of the base material and bolt material, respectively.

The applied bolt is of grade 8.8, while the material is S235, which means that the characteristic value of the yield strength is equal to 640 MPa and 235 MPa for the bolt and the base material, respectively, according to the Eurocode 3 (1993). Generally, these characteristic values are adopted as the basis of further calculations. According to previous experiences, however, a higher value is considered for the base material (270 MPa).

The column section is assumed to be a HEA 200 profile, or similar, the height of which is $h = 190$ mm. For the bolt position and extension of end-plate $m = 40$ mm and $n = 50$ mm are applied. The thickness of the end-plate is treated as a parameter, varying between 10 and 50 mm. The bolt diameter is 16 mm, which gives approximately $A_b = 200$ mm^2 for the area of one bolt.

The calculations are summarised in Table 1, showing the resistances of the various failure modes for the various plate thickness values. The most probable failure mode is the one to which the minimal resistance belongs.

It can be seen from Table 1 that pure bolt failure is not realistic to achieve since it occurs only in cases of extremely thick end-plates. For that reason it was decided to eliminate pure bolt failure

Table 1 Moment resistance calculation of the joints

t [mm]	Plate res. [kNm]	Mode 1 [kNm]	Mode 2 [kNm]	Mode 3 [kNm]	Mode 4 [kNm]	Resistance [kNm]
10	1.35	18.1	33.0	55.5	85.2	18.1
12	1.94	27.0	36.3	56.3	85.2	27.0
16	3.45	51.4	44.5	58.3	85.2	44.5
20	5.40	86.4	55.2	60.7	85.2	55.2
22	6.53	108.6	61.5	62.1	85.2	61.5
25	8.43	148.8	72.2	64.3	85.2	64.3
30	12.15	238.1	93.7	68.6	85.2	68.8
40	21.60	540.0	152.0	79.2	85.2	79.2
50	33.75	1147.5	234.7	92.5	85.2	85.2

from the study and, finally, three pieces of end-plates thickness were chosen, according to failure modes 1, 2 and 3. These are:

- t = 12 mm, for Mode 1,
- t = 16 mm, for Mode 2,
- t = 25 mm, for Mode 3.

In addition, it was decided to study the effect of bolt pre-tensioning. It can be assumed, however, that the resistance is not dependent on the pre-loading.

3.3. The specimens

Altogether five specimens were designed. The main characteristics of the specimens are summarised in Table 2. An additional note is that butt welds are applied between the column and the end-plate in order to minimise the risk of weld failure.

3.4. Displacement transducers

To measure the displacements, inductive displacement transducers were used. The number and the position of the transducers were defined so as to get the most possible information on the behaviour, considering also the place required for each transducer, which gives a limitation of their maximal number. Finally, altogether 13 transducers were used. Their arrangement from T1 to T12 is presented in Fig. 6.

Moreover, there is a transducer, not presented in Fig. 6, to measure the horizontal displacement of

Table 2 Specimens main characteristics

Specimen	Column section	End-plate thickness	Bolt tightening	Anticipated behaviour
CB1/CB1R	HEA200	25 mm	hand-tightened	Mode 3
CB2	HEA200	16 mm	hand-tightened	Mode 2
CB3	welded	25 mm	hand-tightened	local buckling
CB4	HEA200	25 mm	pre-tensioned	Mode 3
CB5	HEA200	12 mm	hand-tightened	Mode 1

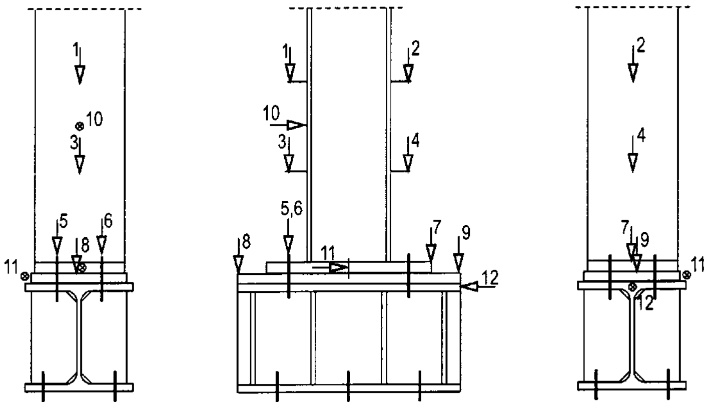

Fig. 6 Arrangement of displacement transducers

Table 3 Loading history

Cycle nr.	1	2	3	4	5	6	7	8	9	10	11	
Displacement amplitude	$\frac{1}{4}e_y$	$\frac{1}{2}e_y$	$\frac{3}{4}e_y$	e_y	$2e_y$	$2e_y$	$3e_y$	$3e_y$	$4e_y$	$4e_y$	$5e_y$	etc.

the load application point. Since all of the test procedurs are controlled by this displacement, it is referred to as transducer T0.

3.5. Loading history

The loading history is defined in accordance with ECCS (1986) on the basis of the displacement belonging to the limit of elasticity (e_y). In this study, however, two cycles were applied in the plastic range instead of three as proposed in the (ECCS 1986), because it was observed in previous tests (Calado and Lamas 1998) that the third cycle does not give additional information relatively to the previous two cycles. The general pattern of the loading is summarised in Table 3.

3.6. Determination of limit of elasticity

Before performing the cyclic test, the yielding displacement (e_y) has to be determined. It can be done by monotonic test, as it is proposed in ECCS (1986), or by preliminary calculations. In this experimental program a finite element simulation was performed, using a model developed by the authors (Dunai and Ádány 1997). As an example, Fig. 7 shows the FE model of CB2, with the applied finite element mesh. Only the bottom part of the specimen was modelled (a 200-mm-high piece of the column), applying prescribed forces on the top of the model.

The calculated moment-rotation curve is presented in Fig. 8. On the basis of the moment-rotation relationship, the force-displacement relationship can be established. From the force-displacement curve the yielding displacement and yielding force was determined according to the ECCS recommendations as it is illustrated in Fig. 8.

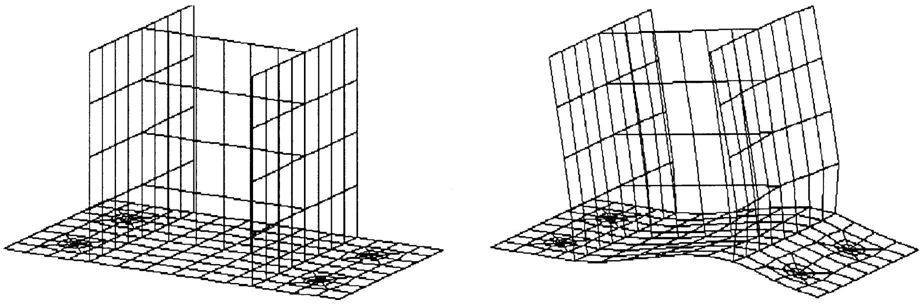

Fig. 7 Undeformed and deformed grid of the FE model for CB2

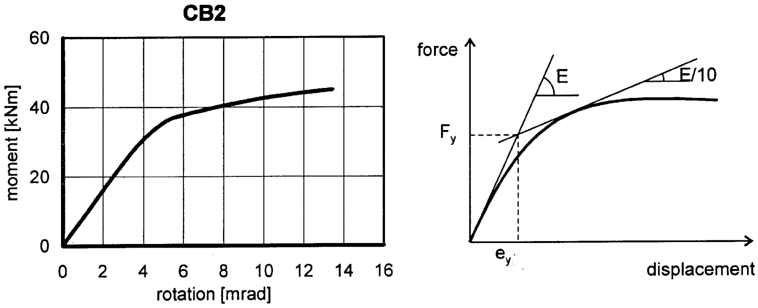

Fig. 8 Calculated monotonic moment-rotation diagram for CB2, and the determination of limit of elasticity

4. Results

4.1. Summary on the tests

At test CB1 (HEA 200 column, 25-mm-thick end-plate, hand-tightened bolts, see Table 2), the governing phenomenon of the behaviour is the elastic-plastic elongation of the bolts. The plastification, however, takes place not in the bolt shank but in the bolt and nut threads. Due to the deterioration of the nut thread, at the end of cycle 7 the nuts of the tensioned bolts had "jumped" from the bolt, which means joint failure.

Since the specimen had not significantly deteriorated during the test it was decided to replace the bolts, applying more nuts (3 pcs), and repeating the test. The repeated test is referred to as CB1R.

In the case of CB1R (see Table 2 and Fig. 9) the behaviour is basically identical with that of CB1, following Mode 3 (see Section 3.2). The most important phenomenon is the bolt elongation, combined with certain end-plate deformation. In this case, however, the bolt plastification takes place in the bolt shank, which results in having more cycles performed. At the end of cycle 13 one of the tensioned bolts broke which means failure of the joint.

In the case of CB2 specimen (HEA 200 column, 16-mm-thick end-plate, hand-tightened bolts, see Table 2 and Fig. 10) specimen, the behaviour follows Mode 2 (see Section 3.2). There is a strong interaction between two basic phenomena: base-plate deformation and bolt elongation. Both components reach its plastic state, due to plate bending for the base-plate, and a combined tension/bending for the bolt. At the very end of cycle 16 the flange weld broke, causing failure of the joint.

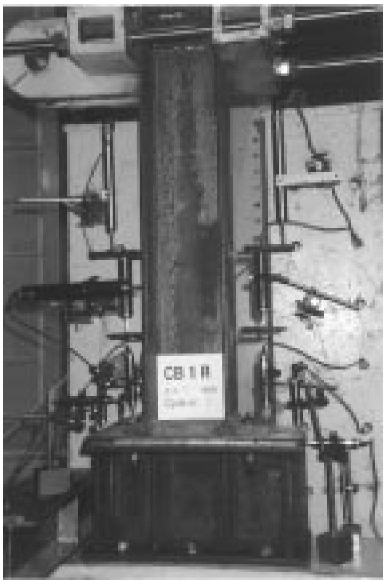

Fig. 9 CB1R test

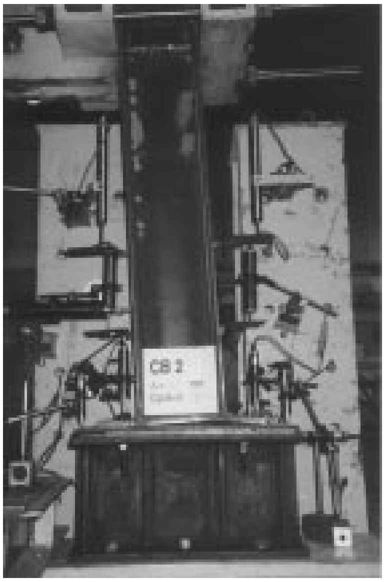

Fig. 10 CB2 test

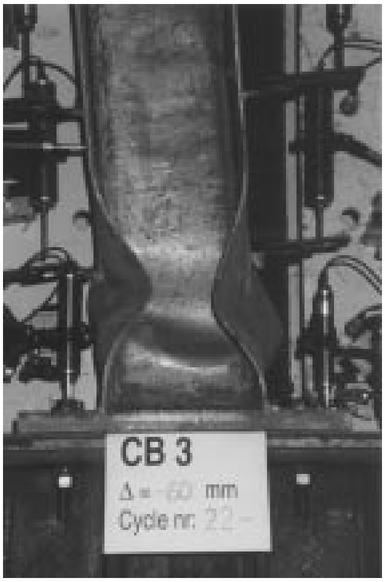

Fig. 11 CB3 test

At CB3 test (welded column, 25-mm-thick end-plate, hand-tightened bolts, see Table 2) the governing phenomenon is the buckling of the column flanges and web, as it can be seen in Fig. 11. There is no considerable deformation of the bolt, and it remains practically elastic during the whole test. Similarly, the base-plate remains practically flat, without plastic deformations. The large deformations are concentrated in the bottom part of the column, approx. 300 mm from the end-plate. It is to be noted that the deformation pattern of the column is not exactly symmetrical. It is interesting to observe that there is a considerable shortening of the column due to the flange/web buckling. (The maximum shortening is approx. 25 mm.) After the 27th cycle, it was decided to stop the test, since the majority of transducers reached their measuring capacity, due to the large deflections.

CB4 specimen (HEA 200 column, 25-mm-thick end-plate, pre-tensioned bolts, see Table 2) is identical with CB1 and CB1R, with only the difference of bolt pre-tensioning. The behaviour is similar to that of CB1R, governed by the bolt elongation. At cycle 11, one of the tensioned bolts is broken, as it is presented in Fig. 12. The test was not continued because of the significant degradation of the joint load-bearing capacity.

For CB5 (HEA 200 column, 12-mm-thick end-plate, hand-tightened bolts, see Table 2) the governing phenomenon is definitely the base-plate deformation (elastic and plastic). Nevertheless, the bolt elongation also has an influence, especially after some plastic cycles. The behaviour is between Mode 1 and Mode 2 (see Section 3.2). Nevertheless, a prying effect was clearly observed, especially at larger displacements.

In cycle 11 a small crack occurred in the end-plate beside the flange weld, along the whole width of the end-plate. At the end of cycle 14 a similar crack developed at the opposite side of the column. The development of the weld cracks resulted in a degradation of the resistance. At cycle 18 the joint failed, caused by a complete failure of the end-plate (see Fig. 13).

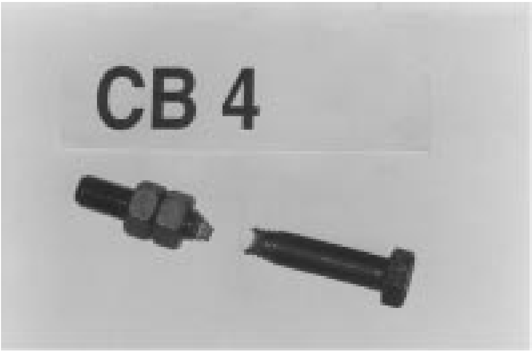

Fig. 12 Failed bolt from CB4 test

Fig. 13 End-plate failure in CB5 test

4.2. Procedure for results evaluation

4.2.1. Definition of the joint reference section

In order to be able to calculate the various mechanical characteristics of the investigated column-base joint, it is necessary to define a section as *joint reference section*. This section is used to measure the forces/moments which act on the joint, and also the displacements of this section give the joint displacements.

The joint reference section is defined at a distance of twice the column section depth ($h_{ref} = 2\times d$) in order not to be disturbed by the intensive deformation due to local buckling. Note that h_{ref} is measured from the top surface of the base-plate, while d is the distance between the system lines of the flanges, as it is illustrated in Fig. 14. Since d is equal to 180 mm for all the specimens, the reference section is situated 360 mm from the base-plate.

4.2.2. Forces, moments

The joint forces/moments are defined as the internal forces/moments of the reference section.

- The bending moment (M) can be calculated as $M = F\cdot\Delta h$, where Δh is the vertical distance between the load application point and the reference section being equal to 530 mm for each specimen, while F is the applied force.
- The shear force (V) of the joint is equal to the force (F) applied to the specimen at the column top.

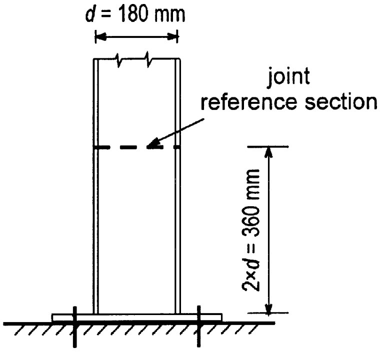

Fig. 14 Joint reference section

4.2.3. Base rotation

The rotation of the base can be calculated from the vertical displacements of the base element as:

$$\Theta_{base} = (t_9 - t_8)/d_{8-9} \tag{9}$$

where t_8 and t_9 are the displacements measured by T8 and T9, and $d_{8\text{-}9}$ is the distance between the two transducers.

4.2.4. Rotation of the reference section

The rotation of the reference section can be calculated from the measured vertical displacements of the flanges, which are recorded at two different levels. The elastic column deformations should also be considered. The rotation calculated from T1-T2 and T3-T4:

$$\Theta_{1-2} = \frac{t_2 - t_1}{d_{1-2}} - \Theta_{1-2}^{el} - \Theta_{base} \tag{10}$$

$$\Theta_{3-4} = \frac{t_4 - t_3}{d_{3-4}} + \Theta_{3-4}^{el} - \Theta_{base} \tag{11}$$

where

t_i is the displacement measured by the *i*-th transducer,

$d_{1\text{-}2}$ and $d_{3\text{-}4}$ are the horizontal distances between transducer T1-T2 and T3-T4, Θ_{base} is the base rotation as defined above, Θ_{1-2}^{el} and Θ_{3-4}^{el} are the elastic rotations between the reference section and measuring point for T1-T2 and T3-T4 transducers, respectively.

The rotation of the reference section is generally determined as the average value of those calculated from T1-T2 and T3-T4.

$$\Theta_{ref} = \frac{\Theta_{1-2} + \Theta_{3-4}}{2} \tag{12}$$

4.2.5. Slip between the base and base-plate

The relative displacement between the base-plate and the base element can be derived from the data measured by T11 and T12, considering the appropriate signs.

$$sl = t_{11} - t_{12} \tag{13}$$

4.2.6. Bolt elongation

The bolt elongation can be determined directly from the displacement measured by T5 and T6. However, it is enough to consider the positive displacements only.

$$el = \frac{t_5 + t_6}{2} \tag{14}$$

4.3. Moment-rotation characteristics

The moment-rotation relationship of the reference section is established on the basis of the measured displacements, according to the formulae presented in Section 4.2. The moment-rotation curves are presented in Fig. 15.

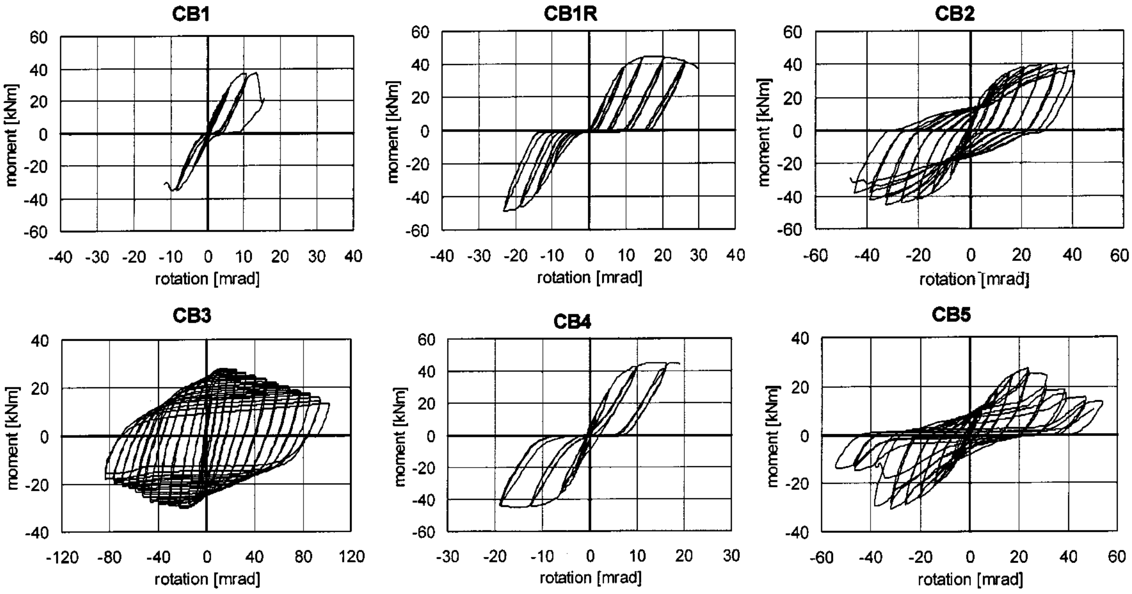

Fig. 15 Moment-rotation diagrams

4.4. Base deformation

A general observation is that the deformations of the base element are not significant. They always remain in the elastic domain, with a maximum rotation of approx. 2-2.5 mrad, and a maximum horizontal displacement of approx. 1 mm. Note that the yielding rotation is between 4 and 12 mrad, which means that the base deformation has no significant effect in the plastic range, but cannot be neglected in the vicinity of the elastic range.

As an example, Fig. 16 shows the rotation of the base element for CB2 and CB3. Similar diagrams are obtained for all the specimens, which clearly demonstrates that the base deformations are elastic, without having considerable effect on cyclic joint behaviour.

4.5. Slip between the base and base-plate

Fig. 17 shows the slip-force diagram for the CB2 and CB3 specimens. Here, the term "force" is

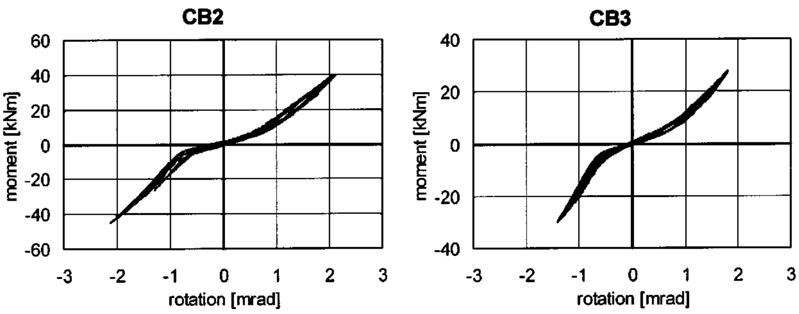

Fig. 16 Rotation of the base element in the cases of CB2 and CB3 tests

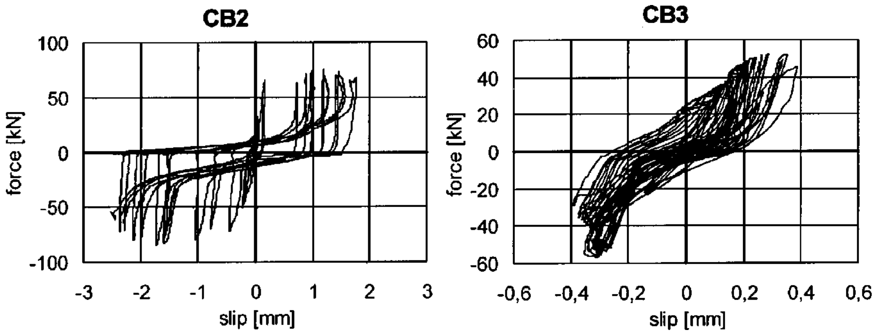

Fig. 17 Slip between the base and base-plate for CB2 and CB3

the shear force. It can be observed that the development of the slip begins at the zero-force level of each cycle, and very rapidly reaches its maximum value. This observation can be easily explained by taking into consideration that, at the zero-force level, the contact area between the base-plate and the base element is reduced due to the residual deformations of the base-plate.

Similar diagrams can be obtained for all the cases where significant base-plate or bolt deformation is experienced (CB1, CB1R, CB2, CB4, and CB5). However, in the case of CB3, the effect of slip is almost negligible, since the base-plate and the bolts are not subjected to plastic deformations.

4.6. Bolt elongation

Fig. 18 presents the bolt elongation in the cases of CB2 and CB3 specimens. The diagram which was obtained for the CB2 test demonstrates well the yielding of the bolts, as well as the significant residual deformations. Similar diagram can be shown for CB1R and CB4, too, where considerable bolt elongation occurred due to plastic deformations. In the cases of CB3 and CB5, however, the bolts remain practically elastic; consequently, there are no large deformations, nor residual displacements.

4.7. Cyclic characteristics

The moment-rotation curve, being the most important cyclic curve of the investigated type of

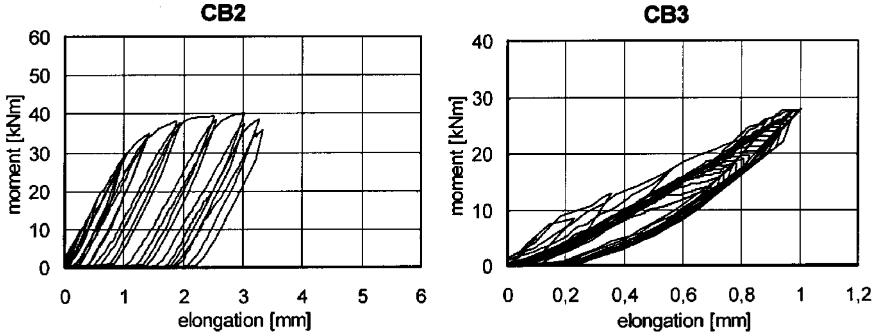

Fig. 18 Bolt elongation for CB2 and CB3

Table 4 Formulae for calculation of cyclic parameters

	Positive hemicycles	Negative hemicycles
Partial ductility	$\mu_{0i}^{+} = \dfrac{\Theta_i^{+}}{\Theta_y^{+}}$	$\mu_{0i}^{-} = \dfrac{\Theta_i^{-}}{\Theta_y^{-}}$
Full ductility ratios	$\psi_i^{+} = \dfrac{\Delta\Theta_i^{+}}{\Theta_i^{+} + \Theta_i^{-} - \Theta_y^{-}}$	$\psi_i^{-} = \dfrac{\Delta\Theta_i^{-}}{\Theta_i^{-} + \Theta_i^{+} - \Theta_y^{+}}$
Resistance ratios	$\varepsilon_i^{+} = \dfrac{M_i^{+}}{M_y^{+}}$	$\varepsilon_i^{-} = \dfrac{M_i^{-}}{M_y^{-}}$
Rigidity ratios	$\xi_i^{+} = \dfrac{tg\alpha_i^{+}}{tg\alpha_y^{+}}$	$\xi_i^{-} = \dfrac{tg\alpha_i^{-}}{tg\alpha_y^{-}}$
Absorbed energy ratios	$\eta_i^{+} = \dfrac{A_i^{+}}{M_y^{+} \cdot (\Theta_i^{+} - \Theta_y^{+} + \Theta_i^{-} - \Theta_y^{-})}$	$\eta_i^{-} = \dfrac{A_i^{-}}{M_y^{-} \cdot (\Theta_i^{+} - \Theta_y^{+} + \Theta_i^{-} - \Theta_y^{-})}$

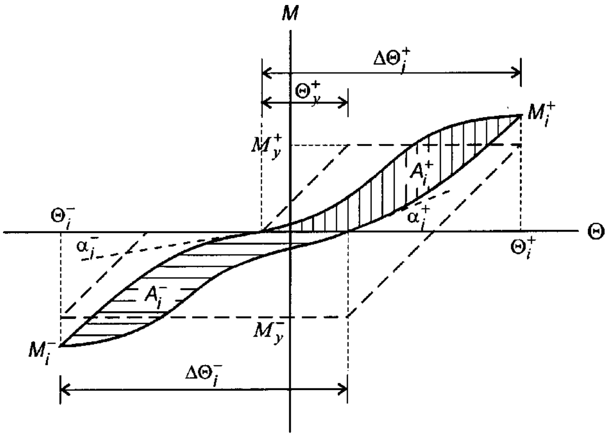

Fig. 19 Notation for the calculation of cyclic characteristics

joint, is chosen to establish the cyclic characteristics, as it is proposed in ECCS (1986). Four parameters are calculated: the *full ductility ratio*, the *resistance ratio*, the *rigidity ratio* and the *absorbed energy ratio*. In the following, these ratios are plotted as a function of the *partial ductility.* The formulae are presented in Table 4, according to the notations of Fig. 19.

The calculated cyclic parameters are presented in Fig. 20 for the positive hemicycles of the moment-rotation diagrams. Note that the CB1 test is not evaluated here, since, due to the early failure of the bolt and nut thread, the loading history is too short.

4.7.1. Effect of bolt pre-tensioning

The CB1R and CB4 specimens are identical. However, in the case of CB1R, the bolts are hand-tightened, while in the case of CB4, pre-tensioning is applied. Thus, the effect of bolt pre-tensioning can be analysed by comparing the two cases.

The behaviours observed during the two tests are similar, and the calculated cyclic parameters

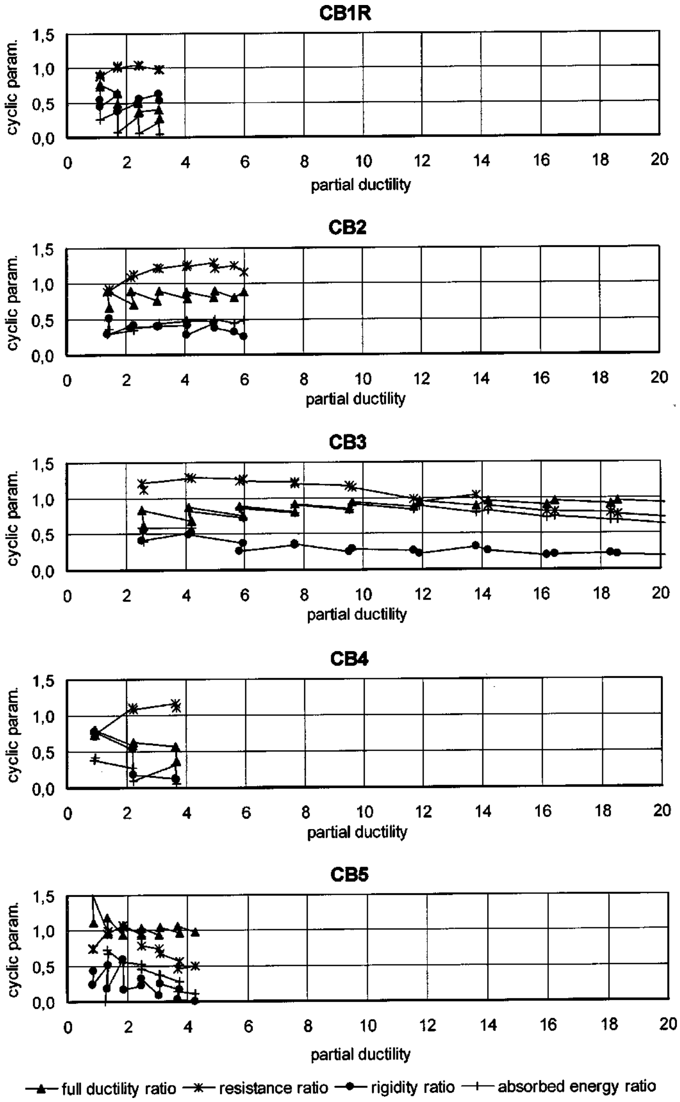

Fig. 20 Cyclic characteristics for positive hemicycles of moment-rotation curves

have similar tendencies as well as, according to Fig. 20. Thus, it can be stated that the bolt pre-tensioning has no important effect on the cyclic behaviour in the analysed cases.

4.7.2. Deformation capacity

An important observation is that the deformation capacities of the various tested joints strongly differ from each other.

- If the governing behaviour is the bolt behaviour (Mode 3, see CB4 or CB1R), the maximal value of the partial ductility is approximately. equal to 4. In this case the failure of the specimen is caused by the failure of the bolts. Since the bolts are of high-strength steel, the deformation capacity of the bolts is limited, which results in a small deformation capacity of the joint.

- In the case of CB2, there is a strong interaction between the bolt and end-plate (Mode 2). The maximal value of the partial ductility is 6. In this case the failure is caused by the crack which occurred at the flange to end-plate welds. It means that although the behaviour itself is governed by the end-plate and bolt deformations, the failure is caused by the weld crack, which limits the deformation capacity of the joint.
- CB 5 corresponds to Mode 1, when the behaviour is basically governed by the end-plate deformations. The maximal partial ductility is slightly more than 4. It is to be noted, however, that the failure is caused by the failure of the flange weld again, which reduced the deformation capacity.
- If the governing behaviour is the column flange/web buckling (CB3), the maximal partial ductility is much greater than any of the other cases (more than 20). Moreover, it should be mentioned that the CB3 joint did not reach its deformation capacity during the test. (The test was finished because of the measuring devices.)

4.7.3. Ductility

In the case of bolt behaviour (CB4), full ductility ratio is rapidly decreasing during the consecutive cycles. This degradation is in connection with the rigid-body-type rotation of the joint, as it is described later.

In the other cases the value of the full ductility ratio is near to 1, which corresponds to ductile behaviour.

4.7.4. Resistance

Generally it can be stated that all the cases represent good cyclic behaviour from the viewpoint of resistance. The value of the resistance ratio is usually more than 1, without considerable degradation, which means that the moment resistance of the joint does not change significantly even after several plastic cycles of loading.

The only exception is the case of the end-plate behaviour (CB5). In this case the decreasing tendency is definitely caused by the flange weld crack, which resulted in a reduced end-plate cross-section at the welds, and consequently, a reduced resistance of the end-plate and the joint.

4.7.5. Rigidity

In practically all the cases considerable rigidity degradation can be observed.

In the case of governing bolt behaviour (CB4, CB1R) a rigid-body-type rotation clearly can be observed in the moment-rotation diagram. Practically, it means the horizontal part of the diagram at the zero force level.

When the bolt behaviour is combined with the end-plate behaviour, the rigid-body-type rotation does not occur. However, the rigidity is strongly reduced.

From a rigidity point of view, CB3 shows the best behaviour. There is no rigid-body-type rotation at all, although the rigidity is continuously decreasing due to the deterioration of the whole column section.

4.7.6. Absorbed energy

In the case of governing bolt behaviour (CB1R, CB4) the absorbed energy ratio rapidly decreases during the consecutive cycles. Another important observation that in the repeated cycles (with the same maximal displacement) there is a significant drop of the ratio, which indicates that there is almost no energy dissipation in these repeated cycles. The phenomenon can be traced back to the rigid-body-type displacement, as discussed above.

In the case of CB2 (combined end-plate and bolt behaviour) the value of the absorbed energy ratio is approx. equal to 0.5, constantly. The important thing is that there is no degradation, in this case.

The diagram for CB5 shows a decreasing tendency. This degradation is certainly caused by the weld cracks, which reduced the area of the end-plate, resulting in reduced moment resistance and energy dissipation capacity.

The most advantageous behaviour belongs to CB3, when the local buckling of column flanges/ web determine the behaviour. Even after several plastic cycles the absorbed energy ratio is more than 0.5, although it has a decreasing tendency if the partial ductility is greater than 10-12.

5. Conclusions

In this paper an experimental program on steel bolted end-plate joints is presented with the primary aim of providing information on the behavioural components which determine the joint behaviour. Here, some general conclusions are drawn.

It can be stated that the experimental behaviour of each specimen is in accordance with the expected behaviour. Thus, the applied method for the preliminary calculation is justified. The five different specimens cover a wide range of behaviour, including governing bolt behaviour (CB1 and CB4), governing base-plate behaviour (CB5), column local buckling (CB3) and a combined base-plate/bolt behaviour (CB2).

The tests justified the existence of the three basic types of behaviour. (Note that the concrete behaviour was not investigated in the present study.) However, the important effect of weld cracks is also highlighted. Whenever there is intensive end-plate deformation the failure is caused by the cracks that occurred at the flange to end-plate welds. The cracks also influence the cyclic characteristics causing significant degradation of the moment resistance and the energy absorption capacity. Thus, although the end-plate behaviour would have good cyclic characteristics (since it is determined by the steel material behaviour), the weld cracks can strongly modify the behaviour.

The most advantageous behaviour is experienced if the deformations are concentrated in the column section, forming a plastic hinge (CB3, governing column behaviour). In this case the behaviour is extremely ductile, with considerable energy absorption capacity. On the other hand, whenever there is significant bolt elongation, the rigidity and energy dissipation capacity of the joint considerably decrease, due to the rigid-body-type rotation of the joint. In this case the deformation capacity is also reduced, as a consequence of the limited elongation capacity of the bolts.

The obtained results are applicable for the verification and calibration of numerical models. Detailed experimental data are provided for various behaviour types corresponding to the same joint topology. It is important, however, to study concrete behaviour, which can be the topic of further investigations.

Acknowledgements

The research work has been conducted under the financial support of the following projects: OTKA T020738 (Hungarian National Scientific Research Foundation), PBICT/P/CEG/2359/95 (Fundação para a Ciência e a Tecnologica, in Portugal), and TEMPUS JEP 11236/96.

References

Ádány, S. and Dunai, L. (1995), "Rigidity of column-base connections under combined loading", *International Colloquium on Stability of Steel Structures*, September 21-23, Budapest, Hungary, Preliminary Report, **II**, 3-10.

Ádány, S. and Dunai, L. (1997), "Modelling of steel-to-concrete end-plate connections under monotonic and cyclic loading", *Periodica Politechnica ser. Civil Eng.*, **41**(1), 3-16, 1997.

Ballio, G., Calado, L. and Castiglioni, C. A. (1997), "Low cycle fatigue behaviour of structural steel members and connections", *Fatigue & Fracture of Engineering Materials & Structures*, **20**(8), 1129-1146.

Calado, L., Bernuzzi, C. and Castiglioni, C. A. (1998), "Structural steel components under low-cycle fatigue: design assisted by testing", *Structural Engineering World Congress*, SEWC´98, San Francisco, Paper nº T196-4.

Calado, L. and Lamas, A. (1998), "Seismic modelling and behaviour of steel beam-to-column connections", *Second World Conference on Steel Construction*, San Sebastian, Spain.

Calado, L. and Mele, E. (1999), "Experimental research program on steel beam-to-column connections", *Report ICIST*, DT 1/99.

Calado, L., Mele, E. and De Luca, A. (1999), "Cyclic behaviour of steel semirigid beam-to-column connections", *to be published in ASCE*.

Dunai, L. (1992), "Modelling of cyclic behaviour of steel semi-rigid connection", *First State-of-the-Art Workshop on Semi-Rigid Behaviour of Civil Engineering Structural Connections: COST C1*, Brussels, 394-405.

Dunai, L., Ádány, S. and Fukumoto, Y. (1995), "Moment-rotation model of steel-to-concrete end-plate connections", *Third International Workshop on Connections in Steel Structures*, 29 May - 1 June, Trento, Italy, Connections in Steel Structures III, ed. R. Bjorhovde, A. Colson and R. Zandonini, 269-277.

Dunai, L., Fukumoto, Y. and Ohtani, Y. (1996), "Behaviour of steel-to-concrete connections under combined axial force and cyclic bending", *Journal of Constructional Steel Research*, **36**(2), 121-147.

Dunai, L. and Ádány, S. (1997), "Cyclic deterioration model for steel-to-concrete joints", *Second International Conference on the Behaviour of Steel Structures in Seismic Areas* (STESSA '97), August 3-8, Kyoto, Japan, ed. F. M. Mazzolani, H. Akiyama, 564-571.

ECCS (1986), "Recommended testing procedure for assessing the behaviour of structural steel elements under cyclic loads", *Technical Committee 1*, TWG 1.3, 45.

Eurocode 3 (1993), "Design rules for steel structures, part 1, general rules and rules for buildings", ENV 1993-1-1.

Ferreira, J. (1994), "Characterisation of the behaviour of semi-rigid steel connections", MSc Thesis, Instituto Superior Técnico, Lisbon, Portugal (*in portuguese*).

Wald, F. (1994), "Connection design tables to ENV 1993-1-1 (Eurocode 3)", *ed*: Wald, F., Prague.